A temporal Convolutional Network for EMG compressed sensing reconstruction

A Temporal Convolutional Network for EMG Compressed Sensing Reconstruction

Abstract

Electromyography (EMG) plays a vital role in detecting medical abnormalities and analyzing the biomechanics of human or animal movements. However, long-term EMG signal monitoring will increase the bandwidth requirements and transmission system burden. Compressed sensing (CS) is attractive for resource-limited EMG signal monitoring. However, traditional CS reconstruction algorithms require prior knowledge of the signal, and the reconstruction process is inefficient. To solve this problem, this paper proposed a reconstruction algorithm based on deep learning, which combines the Temporal Convolutional Network (TCN) and the fully connected layer to learn the mapping relationship between the compressed measurement value and the original signal, and it has been verified in the Ninapro database. The results show that, for the same subject, compared with the traditional reconstruction algorithms orthogonal matching pursuit (OMP), basis pursuit (BP), and Modified Compressive Sampling Matching Pursuit (MCo), the reconstruction quality and efficiency of the proposed method is significantly improved under various compression ratios (CR).

Keywords: Electromyography; Compressed Sensing; Temporal Convolutional Network; Reconstruction

1. Introduction

The health detection system [1] has gradually formed a trend of collecting the physiological signals of the human body with small and portable biosensors. It transmits the data wirelessly through the central node to the telemedicine center and provides it to doctors for data analysis and medical diagnosis. The monitoring system has less load and impact on the human body and can implement real-time monitoring through continuous and uninterrupted signal transmission.

As a bioelectrical signal, EMG can be processed to detect medical abnormalities, activation levels, recruitment orders, or the biomechanics of human movement [2]. Catacora et al. [3] proposed a novel dual differential amplifier for electromyography (EMG) measurement, which uses only three electrodes to measure sEMG signals and is suitable for portable and wearable systems. Charn et al. [4] proposed a capacitive electromyography monitoring system that overcomes the limitations of contact electromyography monitoring systems by using capacitive sensing methods. However, long-term EMG monitoring will generate large data storage, and wireless transmission will consume vast energy for real-time monitoring signals [5, 6]. Therefore, compressing EMG signals is needed to reduce energy consumption. Discrete wavelet transform [7, 8, 9], discrete cosine transform [10, 11, 12], discrete fourier transform [13] and other lossy compression techniques based on domain transform are widely used in signal compression. However, these methods are based on fully sampled signals, which is inefficient [14]. In addition, the sampling frequency in Nyquist sampling [15] must be greater than twice the maximum frequency of the sampling signal to accurately recover the original signal, which will lead to a waste of resources.

As an emerging data compression technology, compressed sensing (CS) [16] solves this problem well. It performs linear measurements on the original signal through under-sampling technology [17] and reconstructs it using several measured values. Therefore, CS can be applied to remote EMG monitoring. Since compression is a simple linear operation, the complexity of the calculation at the acquisition end can be reduced.

The CS theory mainly includes three aspects. The first aspect is to analyze the sparsity of the signal. The sparsity of the compressed signal is a prerequisite for applying compressed sensing technology. However, in practical applications, there are very few signals sparse in the time domain, so there is research on signal sparsity. Most signals that are not sparse in the time domain can be transformed into sparse ones in other domains. The commonly used sparse basis is the Fourier orthonormal basis, discrete cosine orthonormal basis, wavelet orthonormal basis,*etc.* The second aspect is the design of the measurement matrix. When the measurement matrix compresses the original data, it retains the original signal's core information and reduces the signal's data volume. The measurement matrices can be either a random measurement matrix or a deterministic measurement matrix. The advantage of the random Gaussian matrix and the random Bernoulli matrix is that they can satisfy Restricted Isometry Property (RIP) [18] with

overwhelming probability. RIP is a beneficial condition that ensures good recovery performance. The deterministic-based measurement matrices are very useful because random matrices require embedded microcontrollers equipped with floating-point units to perform operations with floating-point numbers. If the measurement matrix is deterministic, the embedded microcontrollers do not need to generate or store random numbers, so the encoder is simple. The third aspect is the selection of the reconstruction algorithm. The function of the reconstruction algorithm is to reconstruct the original signal according to the original signal information contained in the compressed measurement value. So far, the commonly used reconstruction algorithms mainly fall into three categories: convex optimization algorithm, greedy algorithm, and combination algorithm.

As an algorithm with high reconstruction accuracy, the convex optimization algorithm transforms the solving of non-convex optimization into convex optimization. It uses the minimized norm instead of the norm. The most commonly applied convex optimization algorithm is basis pursuit (BP) [19]. The greedy algorithm orthogonalizes the new atoms generated after the iteration, and the least square method is employed to approximate the optimal solution of the original signal. It reduces the number of iterations and accelerates the convergence, and its representative algorithm is the Orthogonal Matching Pursuit (OMP) [20]. Compared with convex optimization algorithms, it simplifies the operation at the loss of reconstruction accuracy. Nowadays, some greedy class reconstruction algorithms have the same accuracy as convex optimization, such as subspace pursuit(SP) [21]. The combination algorithm reconstructs the original signal through the grouping test of the signal. Although the calculation of this type of algorithm is simple, the reconstruction accuracy is low, leading to relatively little research and application. These algorithms are based on sparse prior knowledge and reconstruct the original signal by solving the optimization problem. However, CS cannot be used for real-time reconstruction since the solution is iterative and hence time-consuming [22].

Currently, the research on the compression and reconstruction of EMG signals is less than that on EEG and ECG. Casson et al. [23] explored the compression sensing performance of EMG signals. They calculated the recovery of the EMG signal under various CR. However, compared with the original signal, the PRD value is at least 50%. The calculation results show that several traditional reconstruction algorithms cannot reconstruct good EMG signals. Darren et al. [14] do not recommend using compressed sens-

ing to collect EMG signals because of the poor reconstruction quality of EMG signals. Dixon et al. studied EMG signals' compression performance. Their experimental results show that a 1-bit Bernoulli measurement matrix can produce up to sixteen compressions for EMG biosignals [24]. Bharat Lal et al. [25] summarized the recent research on compressed sensing of EMG signals, including the advantages and disadvantages of sensing matrix, sparse basis, and reconstruction algorithms. The article mentions an Analog-based CS architecture proposed by Mo et al. [26] , which consists of three novel algorithms for the design and implementation of wearable wireless sEMG biosensors, achieving PRD=24% at CR of 60%. Balouchestani et al. proposed using a K-means clustering algorithm [27] and compressed sensing to improve the classification speed of healthy people, people with muscle lesions, and people with neuropathy. Krishnan et al. proposed a simulation-based CS algorithm [2] the transmitter of wearable and wireless biosensors to prevent the loss of important information in the case of high CR. Zhang et al. [28] conducted a study on the compression perception performance of EMG signals using 52 different wavelet bases and five traditional reconstruction algorithms. They found that the db2 wavelet bases and the BP reconstruction algorithm were the most suitable for EMG signals. However, the reconstruction accuracy still needs to be improved. Lorenzo Manoni et al. [29] presented a comprehensive comparative study of computational methods for CS reconstruction of EMG signals. They compared three sparse bases, DCT (Discrete Cosine Transform), HAAR, and DB4, as well as four reconstruction algorithms, ℓ_1, OMP, CoSaMP, and NIHT. The results showed that the DB4 wavelet basis had advantages, while ℓ_1 reconstruction algorithm had the most accurate reconstruction quality and the least reconstruction time. Chen et al. [30] explored the compressive sensing performance of EMG signals. Studies have shown that EMG is not sparse in the time domain, and is sparser in the wavelet domain than DCT and DFT (Discrete Fourier Transform). In addition, the Bernoulli matrix is less computationally complex than the Gaussian matrix, so the Bernoulli matrix is selected as the measurement matrix of the EMG signals. Based on the CoSaMP algorithm, they proposed an modified CoSaMP algorithm, which obtained a reconstruction quality similar to that of the BP reconstruction algorithm. In summary, most studies suggest that the traditional reconstruction algorithm is unsuitable for EMG signal reconstruction.

Currently, some researchers have applied deep learning to reconstruct ECG signals. Hong et al. [31] proposed a deep learning reconstruction al-

gorithm combined with a convolutional neural network (CNN) and a long short-term memory (LSTM) network that is applied to the recovery process of an ECG signal. Specifically, firstly, the ECG signal is synchronously sampled and compressed using the measurement matrix. Then the compressed signal is transposed and projected to ensure that the transposed projection signal has the same size as the original ECG signal. Then, CNN is used to learn the mapping relationship between the transposed projection signal and the original signal to initially reconstruct the ECG signal. Finally, the signal reconstructed by CNN is rebuilt twice by LSTM. Compared with the traditional algorithm, it improves the accuracy of the signal under each CR and the reconstruction efficiency. Mangia et al. [32] reconstructed ECG and EEG using a deep neural network. However, their method depends on the sparsity of physiological signals, and the result is different from the actual reconstructed signal, which needs reprocessing. Muduli et al. [33] proposed a method of using deep learning to compress and recover the fetal electrocardiogram signal, improving the remote monitoring system's calculation speed and obtaining good reconstruction quality.

In recent years, the Temporal Convolutional Network (TCN) [34] has been applied in the field of EMG signals. In the prediction, recognition and classification of EMG, TCN can be used to train and test the model together with the corresponding labels. The trained model can be used to automatically identify different muscle activities or movement types, thus playing an important role in medical, rehabilitation, motion analysis and other applications. In paper [35], it was demonstrated that an encoder-decoder temporal convolutional network model can provide predictions that are both more consistent and precise compared to alternative framewise or sequential models when analyzing EMG signals. Joseph et al. [36] compared the TCN with other state-of-the-art methods and proved that the use of temporal convolutional networks has better accuracy and stability for the classification of EMG signals. Panagiotis et al. [37] applied temporal convolutional networks for electromyography-based gesture recognition as a sequence classification problem. The proposed network outperforms the state-of-the-art reported in the literature by nearly 5% in gesture recognition.

To solve the problem that traditional reconstruction methods are unsuitable for EMG, inspired by the deep learning reconstruction algorithm of ECG signals, we explored a data-driven deep learning method to reconstruct the compressed EMG signals without considering any prior information about EMG. Specifically, we multiplied the original EMG signals with the mea-

surement matrix to obtain the measurement value and then employed a deep learning framework combining TCN and fully connected layers to learn the features and reconstruct the original signal. Since the TCN network does not require prior knowledge of the input signal, we did not use a wavelet sparse basis to decompose the signal. Instead, we directly compressed the EMG signal using the measurement matrix to obtain the measured value, which is applied as the input of the network.

The contributions of this work are mainly in two aspects.

1. A novel EMG CS reconstruction method using a temporal convolutional network and a full connection layer called TCNN is proposed to deal with the main challenges in EMG compressive sensing: Traditional CS reconstruction algorithms do not achieve satisfactory EMG recovery results. Compared with the traditional CS reconstruction algorithm, the reconstruction quality and efficiency of the artificial intelligence algorithm are greatly improved.

2. The reconstruction quality of the proposed network under various CR was tested, and the CR most suitable for EMG signal recovery was obtained according to the reconstruction quality.

The remainder of this paper is structured as follows. In the methods and materials section, the basic concept of CS and the structure of TCN are elaborated. In the results section, the dataset and network configuration used in the experiment are first introduced, and then the calculation results are presented. In the discussion and conclusion section, the experimental results are summarized, the deficiencies are put forward and future implementation plans are formulated.

2. Methods and Materials

As shown in Fig.1, the entire experimental process is shown. Firstly, the original signal is randomly projected to calculate the measured value $\boldsymbol{y}$. Then, the measured value $\boldsymbol{y}$ is reconstructed using OMP, BP, MCo and deep learning frameworks to obtain the reconstructed signal.

2.1. Random projection

The Compressed sensing proposed by Donoho et al. [16] makes full use of the preliminary information that most signals can sparsely represent on a predetermined set of bases, and uses random projection to realize the direct collection of compressed data at a sampling frequency far lower than the

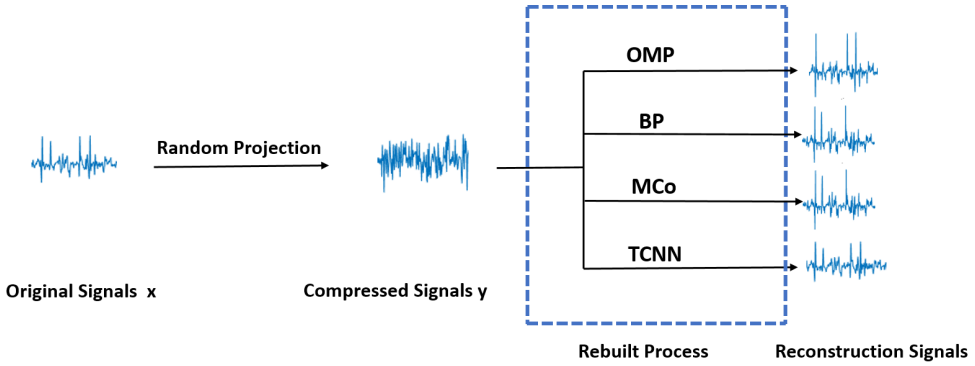

Fig. 1. Model overall

Nyquist frequency. It effectively reduces the sampling frequency and storage space.

Fig.2 shows the CS sampling process, where the sparse signal $\boldsymbol{x}$ to be collected is non-zero only for k times (k is the sparsity), and the remaining points' values are 0 or close to 0. If the signal $\boldsymbol{x}$ is non-sparse in the time domain, it is sparsely decomposed with a specific sparse basis, as shown in formula (1)

$$\boldsymbol{x} = \varphi \boldsymbol{s} \tag{1}$$

where $\boldsymbol{s}$ is the sparse coefficient.

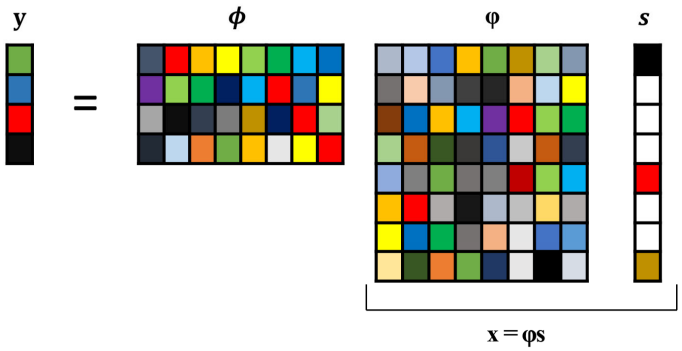

Fig. 2. The CS sampling process

According to the previous research results of Zhang et al. [28], the db2 wavelet base is employed to decompose the EMG signal sparsely, and then it is projected on a given set of sensed waveforms to extract meaningful information in $\boldsymbol{x}$. After that, the measured value $\boldsymbol{y}$ is obtained, as shown in the formula (2)

$$\boldsymbol{y} = \phi \boldsymbol{x} = \phi \varphi \boldsymbol{s} \tag{2}$$

The most commonly used measurement matrices are the Gaussian random matrix and the Bernoulli matrix, which are unrelated to sparse basis. According to the previous work [30, 38, 39], the Bernoulli matrix has lower computational complexity than the Gaussian matrix. Therefore, we choose the Bernoulli matrix as the sensing matrix.

2.2. Reconstruction algorithms

Compressed sensing reconstruction aims to reconstruct the original signal $\boldsymbol{x}$ from the measured value $\boldsymbol{y}$. There is an undetermined problem in solving the original signal from the measured value, but since the signal's sparsity is k, there are only $k+1$ degrees of freedom. Therefore, if the number of measurements exceeds $k+1$ times, the original signal can be recovered nonlinearly.

When any $k+1$ columns of the perception matrix are linearly independent, solve the signal with the sparsest features satisfying the condition of $\boldsymbol{y} = \phi \varphi \boldsymbol{s}$, that is, optimize the following formula

$$min \|\boldsymbol{s}\|_0 \qquad s.t.\ \boldsymbol{y} = \phi \varphi \boldsymbol{s} \tag{3}$$

where $\|\boldsymbol{s}\|_0$ is the number of non-zero values in $\boldsymbol{s}$.

2.2.1. Orthogonal Matching Pursuit

OMP is representative of the greedy algorithm, and Table 1 shows its process. Firstly, the column in the measurement matrix that best matches the signal $\boldsymbol{x}$ is selected to construct a sparse approximation and calculate the signal residual. Then select the column that best matches the signal residual and iterate repeatedly. In each iteration, a Schmidt orthogonalization operation is performed on all selected columns to ensure that the result of each loop is the optimal solution.

Table 1. Pseudocode of Orthogonal Matching Pursuit Algorithm

Algorithm 1 Orthogonal matching pursuit (OMP)	
Input: matrix ϕ,measurements $\boldsymbol{y}$, sparsity K	
Output: sparse reconstruction $\boldsymbol{x}^K$	
Initialization	
$r^0 = \boldsymbol{y}$ and $\Gamma^0 = \emptyset$	
for i=1 ..., K do	
$\lambda^{\mathrm{i}} \Leftarrow argmax_j \lvert\langle \mathrm{r}^{i-1}, \phi_j \rangle\rvert$	Find best fitting column
$\Gamma^i \Leftarrow \Gamma^{i-1} \cup \lambda^i$	
$\boldsymbol{x}^i \Leftarrow argmin_x \lvert\lvert r^{i-1} - \phi_{\Gamma^{\mathrm{i}}} \boldsymbol{x} \rvert\rvert_2$	LS optimization
$\mathrm{r}^i \Leftarrow r^{i-1} - \phi_{\Gamma^{\mathrm{i}}} \boldsymbol{x}^{\mathrm{i}}$	Residual update
end for	

The signal $\boldsymbol{x}$ can be represented by the linear sum of these columns plus the final residual value. In Table 1, the input are ϕ, $\boldsymbol{y}$,K, which represent the measurement matrix, measurement value and sparsity, respectively. In the initialization, r^0 is the residual value, Γ^0 is the index set, and the initial is an empty set $\emptyset$. In the loop, λ is the subscript corresponding to the maximum value of the product of the residual r and the column ϕ_j of the measurement matrix, and then update the index set Γ^i and record the reconstructed atomic set $\phi_{\Gamma^{\mathrm{i}}}$ found in the measurement matrix. Then get $\boldsymbol{x}^{\mathrm{i}}$ by the least square method (LS), and finally update the residual r^{i}. The output is a K-sparse approximation of $\boldsymbol{x}^{\mathrm{k}}$.

2.2.2. Basic pursuit

The essence of CS reconstruction is to solve the underdetermined equation system $\boldsymbol{y} = \phi\varphi\boldsymbol{s}$. This is a zero-norm minimization problem, which is NP-hard (without a fast solution). It can be solved by using the convex optimization method to convert the ℓ_0 minimization to the solution of a ℓ_1 minimization, as shown in the following formula

$$min\|\boldsymbol{s}\|_1 \qquad s.t.\ \boldsymbol{y} = \phi\varphi\boldsymbol{s} \tag{4}$$

As a classical convex optimization method, BP algorithm is applied in this study. Here we use the ℓ_1-magic toolbox [40].

2.2.3. Modified Compressive Sampling Matching Pursuit(MCo)

CoSaMP (Compressive Sampling Matching Pursuit) is an iterative sparse signal recovery algorithm for reconstruction of compressed samples from sparsely represented signals. Chen et al. [30] modified the CoSaMP algorithm and proposed the MCo algorithm. Compared with the CoSaMP algorithm, it improved the reconstruction accuracy of the EMG signal. The algorithm recovers the target signal from a given sampling matrix, noise sample vector and sparsity level. The pseudo-code of MCo is shown in Table 2.

Table 2. Pseudocode of Modified CoSaMP Algorithm

Algorithm 2 Modified CoSaMP(MCo)	
Input: Sampling matrix A, Noisy sample vector u, Sparsity level s	
Output: An s-sparse approximation a of the target signal	
Initialization	
$a_0 \leftarrow 0$, $v \leftarrow u$, $k \leftarrow 0$	
Repeat	
$y \leftarrow A * v$	Form signal proxy
$W \leftarrow supp(y_{2s})$	Identity large components
$T \leftarrow W \cup supp(a_{k-1})$	Merge supports
$b\|T \leftarrow A_T^+ * u$	Signal estimation
$b\|T_c \leftarrow 0$	
$a_k \leftarrow b_s$	Prone approximation
$v \leftarrow u - A * a_k$	Update current samples
When the first type converges	
$P \leftarrow supp(a_{k-1})$	
$W \leftarrow supp(y_{0.5s})$	Signal estimation with smaller set
$T \leftarrow W \cup P$	
$a_k \leftarrow b$	Taking all values
Until halting criterion true	

2.2.4. The temporal convolutional network and full connection layer

The TCN uses dilated causal convolution, which can be used to solve time sequence prediction. It has the following advantages: a. In the training and evaluation stage, unlike the sequential processing of RNN [41], the long input sequence can be processed as a whole in TCN. The training time can be shortened by parallel computing and convolution. b. TCN reduces the problem of gradient explosion and gradient vanishing. c. TCN changes the

size of its receptive field by stacking more expansive (causal) convolution layers and using larger expansion factors. Therefore, TCN can reduce the memory required by the model.

(1) Dilated causal convolution

The purpose of the causal convolution layer in the TCN is to obtain important information from historical data. Fig.3 is the causal convolution in the TCN architecture. It can be seen that the value at time t of each layer only depends on the input value at time t and before time t of the previous layer. The definition of one-dimensional discrete convolution is as follows

$$y(k) = h(k) * x(k) = \sum_{i=0}^{N} h(k-i)x(i) \tag{5}$$

where x and y are the input and output of the network, respectively, * is the convolution operator, and h is the kernel function used for convolution. Each layer adopts zero padding at the edge, which retains the boundary information and makes the input dimension and output dimension of the convolutional layer consistent.

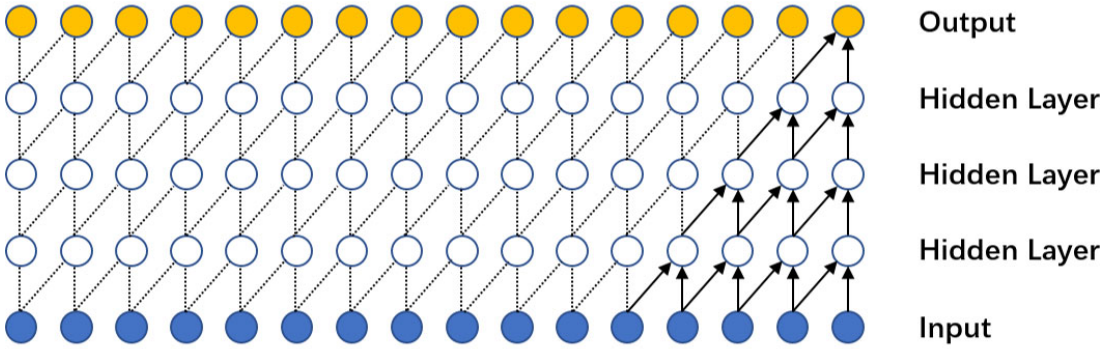

Fig. 3. Visualization of a stack of causal convolutional layers

The dilated convolution adds a dilation into the standard convolution to increase the receptive field and capture more features in the long historical time sequence and information. The dilated convolution has one more hyper-parameter, the partition rate, which refers to the number of intervals in the kernel.In particular, for a one-dimensional time series $X = (x_1, x_2, ..., x_T)$ and

filter f$(0, 1,..., \mathrm{k}-1) \rightarrow \mathrm{R}$, the dilated convolution operation F on element s of the sequence is defined as

$$F(s) = (X * f)(s) = \sum_{i=0}^{\mathrm{k}-1} f(i) \bullet x_{s-d \bullet i} \tag{6}$$

where d is the dilation factor, * is the convolution operator, k represents the size of the filter, and $s - d \bullet i$ accounts for the direction of the past.

Fig.4 is a schematic diagram of causal dilated convolution. Each layer extracts the information of the previous layer in a skipping manner. The expansion factor d increases with an exponential of 2 layer by layer as the network layer increases, which can ensure that the convolution kernel can flexibly select the length of historical data information and cover all historical information inputs. If $d = 1$, the causal dilated convolution degenerates into a general causal convolution operation.

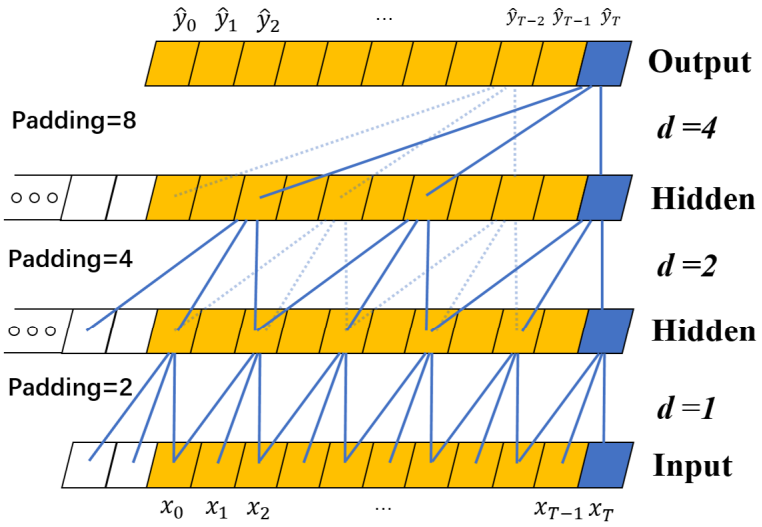

Fig. 4. Visualization of a stack of causal dilated convolution layers

(2) Residual block

Causal dilation convolution makes neural networks complex. Adding residual connections in the output layer of TCN can avoid the problem of gradient disappearance. And residual connections have been proven to be an effective method for training deep networks, which improves the training speed of the network and enables the network to transmit information in a cross-layer manner. It can be expressed as

$$O = Activation(x + F(x)) \tag{7}$$

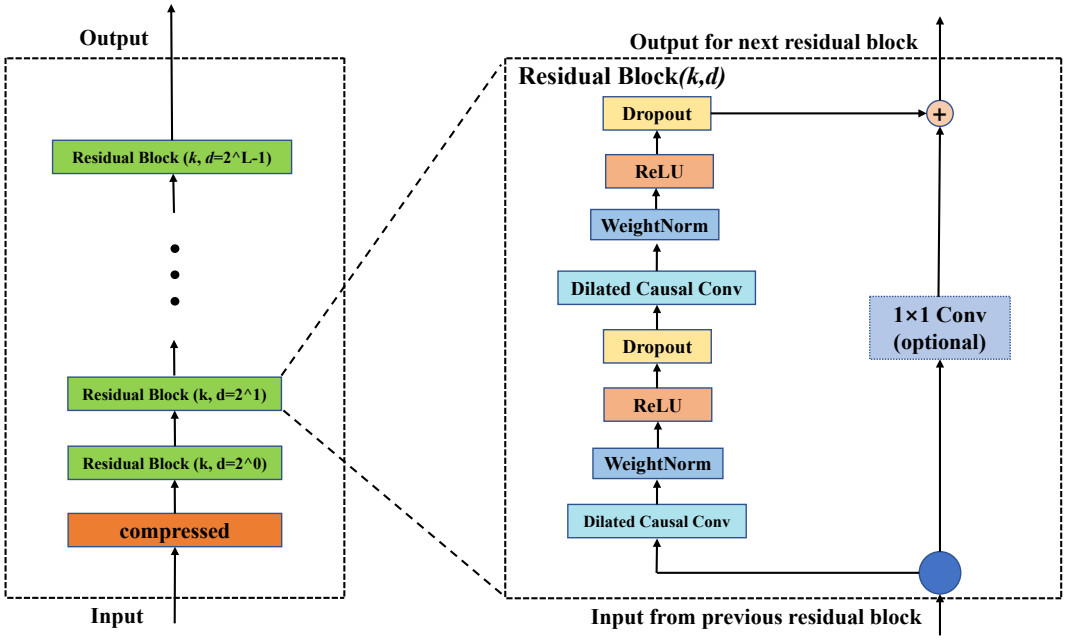

Fig. 5. The structure of the residual block

where O is the output, $F(x)$ represents the residual map to be learned, and the activation function is represented by Activation().

The right part of Fig.5 is the structure of the residual module. Each residual block contains two layers of dilated convolution, weight normalization, and activation function. Here, the Relu is used as the activation function, which can increase the nonlinear relationship between the layers of the neural network and adjust the output value. In addition, a Dropout layer is added after each residual mode convolution to achieve regularization and avoid overfitting. Here, we set the dropout value to 0.5. Since the dimensions between x and $F(x)$ may be different, a 1×1 Conv is designed here to make a simple transformation of x so that the transformed x and $F(x)$ can be added.

TCN makes the input and output the same length. We take 1024 points from the dataset at a time. First, use the 1024×1024-dimensional sparse basis to decompose it, and then the observation matrix is multiplied by the decomposed result. The CR is set to 10%, 30%, 50%, 70%, and 90%, respectively. When CR is 50%, the compressed input data is 512 points, and the result after training by the TCN is also 512 dimensions. In order to get the same 1024 points as the original, it is necessary to make a full connection to

the 512-dimensional data, as shown in Fig.6. It is shown that it is a fully connected layer structure when CR=50% and the same dimension can be obtained by adding a fully connected layer based on the TCN.

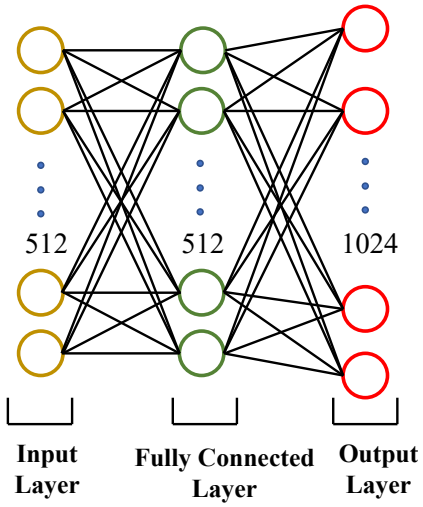

Fig. 6. Full Connection layer when CR=50%

3. Results

In this part, we assess the effect of deep learning on the reconstruction process in EMG compressed sensing. First, we introduce the dataset employed for training and testing and list the evaluation indicators. Next, we present the training details and the hardware configuration used in the calculation. In the end, the reconstruction performance is shown through a series of experiments.

3.1. Description of the EMG datasets

The Ninapro database [42] was applied to verify this experiment's proposed deep-learning reconstruction algorithm. Specifically, we selected the E2 myoelectric signal data of the first eight subjects in the DB2, and the E2 data of each subject includes electromyographic signals collected at 12 electrode positions. Each channel of each subject has over 2 million points of data and the data sampling rate is 2 kHz. Eight subjects included seven men

and one woman, and one of them was left-handed. The specific situation is shown in Table 3.

Since the study by Wu et al. [43] mentioned that the EMG signals measured from different persons are different, and the EMG signals measured from different state of the same individual may be different, we conducted three experiments. The training and test sets used in each experiment are as follows, 1. The first 80% of the data measured by the same subject's electrode at the same position is applied as the training set, and the last 20% is applied as the testing set. 2. Datasets are from different electrodes(DE). The first 80% of the data from the 12th channel of the same subject is used as the training set, and the last 20% of the data from the 2nd channel is used as the test set. 3. Datasets are from different people(DP). The first 80% of the second channel data from different individuals is employed as the training set, and the last 20% is employed as the testing set (The first 80% of the second channel data from the second subject is used as the training set, the last 20% of the second channel data from the first subject is used as the testing set; the first 80% of the second channel data from the third subject is used as the training set, and the last 20% of the second channel data from the second subject is used as the testing set, etc.)

Table 3. Subjects' characteristics.

Parameters	Mean±SD
Age(year)	31.4±5.8
Height(cm)	175.6±10.0
Weight(kg)	72.9±10.9

3.2. Performance indicator

In this research, several performance indicators are employed. CR is utilized to express the compression degree of the signal, which is expressed by formula

$$CR = \frac{M}{N} \times 100\% \tag{8}$$

where N represents the number of points of the original EMG signal, and M is the number of sampling points projected by the measurement matrix. N is

set to a fixed 1024, and the CR is changed by adjusting the value of M. Here, CR of 10%, 30%, 50%, 70%, and 90% are tested. Percentage Root-mean-squared Difference (PRD) is applied to represent the difference between the reconstructed signal and the original signal, and it defined as

$$PRD = \frac{\left\| \hat{X} - X \right\|_2}{\|X\|_2} \cdot 100 \tag{9}$$

where $\hat{X}$ and X are the reconstructed and original signals, respectively. The smaller the value of PRD, the better the reconstruction effect. Signal-to-Noise Ratio (SNR) are utilized to evaluate the quality of signal reconstruction, as defined below

$$SNR = 10\log_{10}\frac{\|X\|_2}{\left\| X - \hat{X} \right\|_2} \tag{10}$$

The coefficient of determination is applied to judge the degree of fit between the reconstructed and actual signals. It is mainly evaluated by R^2 and the formula is

$$R^2 = 1 - \frac{\Sigma_{\mathrm{i}}(\overset{\wedge}{y_i} - y_i)^2}{\Sigma_{\mathrm{i}}(y_i - \bar{y})^2} \tag{11}$$

where y_i represents the value of the ith sampling point of the actual signal, and the corresponding reconstructed signal is represented by $\hat{y}_i$. $\bar{y}$ is the average value of the actual signal. From the above expression, we know that the value range of R^2 is from 0 to 1. The closer it is to 1, the better the model fits the original data.

The correlation coefficient (expressed by r) indicates the degree of linear correlation between two quantities. Its formula is

$$\mathrm{r} = \frac{Cov(X, Y)}{\sqrt{Var[X]Var[Y]}} \tag{12}$$

where $Cov(X, Y)$ is the covariance between X and Y, $Var[X]$ and $Var[Y]$ are the variance of X and Y, respectively. Therefore, r can be expressed as

$$r = \frac{\sum(X_i - \bar{X})(Y_i - \bar{Y})}{\sqrt{\sum(X_i - \bar{X})^2 \sum(Y_i - \bar{Y})^2}} \tag{13}$$

X_i and Y_i represent the ith value of X and Y respectively, and $\bar{X}$, $\bar{Y}$ represent the mean value of X and Y respectively. Generally speaking, the closer r is to 1, the better the correlation between X and Y.

3.3. Training settings and hardware platform

The epoch of the TCN is 500 with a batch size of 16, and the loss function used in training is MSE. The framework is executed on Windows 10 64-bit control system, and the back end is Pytorch. The experiment runs on a laptop with an Intel Core i7-8650u, CPU of 1.9 GHz,16G memory, and 512G hard disk.

3.4. Comparison with traditional reconstruction algorithms

In this part, we compare the deep learning reconstruction algorithm with the traditional greedy algorithm (OMP,MCo)and convex optimization algorithm (BP). Firstly, the reconstruction accuracy of these four algorithms is evaluated by calculating the PRD and SNR between the reconstructed signal and the original signal. Secondly, the difference between the reconstructed and original signals is assessed by calculating R^2 and r. Thirdly, the efficiency of the four reconstruction algorithms is determined by the time of the reconstruction process. Finally, we analyze the reconstructed signals of different methods according to the clinical needs and summarize the CR most suitable for EMG signals.

3.4.1. Reconstruction accuracy evaluation

In this experiment, the PRD and SNR were utilized as index to evaluate the accuracy of the reconstructed signal. We set five CR and calculated the average PRD and SNR of reconstructed EMG signals from eight subjects. The results are shown in Fig.7 and Fig.8. The PRD value and standard deviation in Fig.7 show the signal recovery accuracy of these four reconstruction algorithms under different CR. The deep learning algorithm achieved lower reconstruction error than the other three traditional algorithms when using the same person's data as the training and testing sets (regardless of whether it is data from the same location).

From Fig.8, the signal quality reconstructed by the TCNN is better than the other three reconstruction algorithms under various compression ratios when the training and testing sets are from the same subject. As expected, the rebuild signal loss dropped following the TCNN implementation. However, the reconstruction quality of DL (DP) is not as good as traditional

reconstruction algorithms in all CR, and even performs worse. Furthermore, three traditional algorithms for reconstructing the EMG signal at CR = 50% for 0.5 seconds in record 1 are shown in Fig.9. It can be seen from the comparison between the reconstructed signal and the original signal that the signal waveform through TCNN reconstruction is more similar to the original signal. Therefore, the TCNN is superior to traditional methods when the model is employed for the same position of the subject.

3.4.2. Coefficient of determination and correlation coefficient of the reconstructed signal

To judge the correlation between the reconstructed signal and the original signal, we calculate the coefficient of determination and correlation coefficient between the reconstructed signal and the original signal.

As shown in Fig.10 and Fig.11, it is the histogram of the average value of two parameters under each CR. It can be seen that the two parameters increase with the increase of CR. Under the same CR, the R^2 and r values of DL and DL(DE) are significantly higher than those of the other three algorithms, which shows that the signal reconstructed by the TCNN reconstruction algorithm is closer to the original signals. Therefore, TCNN outperforms traditional methods when the test set data and training set data come from the same person. However, the performance of DL (DP) was not satisfactory.

3.4.3. Evaluation of reconstruction efficiency

When many EMG signals are collected, the reconstruction efficiency of compressed sensing is a crucial factor. We evaluate the computational efficiency of the three reconstruction algorithms by calculating the average reconstruction time of eight data groups under each CR (each data group is about 10 minutes). The specific consumption time is listed in Table 4. Under each CR, the TCNN (test) method's reconstruction time of EMG signals is significantly shorter than that of the other three reconstruction algorithms. Additionally, the TCNN model has float32 parameters of 0.47MB, 1.27MB, 2.07MB, 2.86MB, and 3.67MB at CR of 10%, 30%, 50%, 70%, and 90%, respectively. As expected, the TCNN performs speedily and dramatically improves efficiency.

Table 4. Time (in seconds) of four algorithms for reconstructing a record (about 10 min).

Reconstrction	CR				
Algorithm	10%	30%	50%	70%	90%
OMP	318.54±55.42	310.03±64.80	331.27±71.29	341.46±81.86	360.78±83.82
BP	58.58±16.74	64.99±18.49	75.41±24.44	237.62±70.65	238.32±35.52
TCNN(train)	349.98±37.20	498.96±47.92	530.09 ±48.29	588.68 ±77.07	639.68 ±94.31
TCNN(test)	0.7±0.06	2.21±0.63	3.57±1.20	3.92±1.17	3.93±0.59
MCo	381.34±79.7	420.48±68.4	426.77±109.2	460.97±110.5	757.64±176.1

3.4.4. CR applicable to EMG signals

The quality of EMG signal acquisition determines its value in clinical applications. Zigel et al. [44] evaluated the value of the signal in the clinical application according to different ranges of PRD values. Specifically, when the value of PRD is less than 9, it can be considered that the reconstructed signal has good quality. Based on the previous research, we take PRD = 9 as the evaluation standard and determine the lowest CR suitable for the EMG signals. When PRD=9, each TCNN, OMP, BP and MCo corresponding CR record in the dataset is shown in Table 5.

Table 5. Optimal CR of different methods for PRD = 9.

Data	TCNN	TCNN(DE)	TCNN(DP)	OMP	BP	MCo
1	62.57%	85.20%	95.04%	95.28%	90.30%	89.55%
2	53.51%	74.09%	91.39%	95.78%	88.41%	87.66%
3	52.46%	74.24%	94.17%	94.87%	87.82%	86.83%
4	57.48%	75.23%	92.18%	95.51%	83.39%	82.57%
5	63.31%	91.77%	92.65%	93.62%	67.67%	67.49%
6	60.11%	79.45%	88.81%	93.38%	79.05%	77.89%
7	50.97%	80.27%	92.32%	95.32%	91.41%	90.46%
8	78.89%	92.51%	94.48%	96.31%	91.01%	90.02%
Average	59.91%	81.59%	92.63%	95.01%	84.88%	84.06%

It is evident from Table 5 that the CR of TCNN and TCNN (DE) is lower than the traditional three algorithms, with 59.91% and 81.59%, respectively. This means that in practical application, compared with the tra-

ditional Nyquist sampling method, it will reduce the number of acquisitions by more than 40% and 18%. Meanwhile, BP, OMP, and MCo need more acquisition points to achieve qualified reconstruction quality, and the CR are 95.01%, 84.88% and 84.06%, respectively. Compared with TCNN and TCNN (DE), the other three traditional reconstruction methods increase sampling points by more than 24% and 2.4%. However, the performance of TCNN (DP) is not satisfactory. Although it is better than OMP, it is not as good as the other two reconstruction algorithms.

4. Discussion and Conclusion

Long-term physiological signal acquisition and wireless transmission will depend on a large number of node resources. As an effective physiological signal acquisition method, CS can reduce power consumption and significantly improve the efficiency of physiological signal acquisition. For EMG signals, the researchers have analyzed the compression sampling performance.

Casson et al. [23] used the BP reconstruction algorithm and cubic B-spline dictionary sparse basis to conduct compression sensing sampling test on EMG signals. However, the results showed that EMG signals could not be recovered (the PRD values were above 50 in all cases). Zhang et al. [28] obtained the sparse basis db2 and reconstruction algorithm BP most suitable for EMG signals, but the reconstruction effect is still inaccurate. Mohammadreza et al. [26] presented an analog-based Compressed Sensing (CS) architecture, which consists of three novel algorithms for the design and implementation of wearable wireless EMG biosensors. Compared with Casson et al.'s research, their proposed structure improves the reconstruction effect, achieving a PRD of 24 at a CR of 60%.

This study examined the effectiveness of the depth learning algorithm based on the TCN in the EMG signal compression sensing sampling reconstruction process. It directly learns the mapping relationship between the measured value and the original signals and reconstructs the EMG signal without prior knowledge. The TCNN has been verified in the Ninapro database. When the training set and test set data come from the same measurement location of the same subject, the experimental results show that, compared with the traditional reconstruction method, it significantly improves the reconstruction accuracy at various CR. At the same time, when reconstructing the same signal, TCNN is at least 29 times, 87 times, and 117 times faster than BP, OMP, and MCo algorithms respectively. Therefore,

the TCNN reconstruction algorithm dramatically improves efficiency. From another point of view, the TCNN can achieve good reconstruction quality with a small number of acquisition points. Compared with Nyquist sampling and the other three traditional reconstruction algorithms, TCNN reduces the number of sampling points by more than 40% and 24%, respectively. Compared to the results of others, our proposed TCNN network can achieve a PRD value less than 50 when the CR is over 30%, which has a significant improvement compared to the research results of Casson et al. When the CR is 50%, PRD=15.7 can be achieved, which improves the reconstruction effect while reducing the collection volume compared to the results of Mohammadreza et al. When the training and testing sets are from different measurement positions on the same subject, the reconstruction quality of our proposed network is still better than the other three algorithms under each CR, but not as good as the experimental results of the previous dataset. When using datasets from different subjects, the reconstruction quality of our proposed method is not significantly higher than traditional algorithms under certain CR, and even weaker than that of traditional methods. Peter et al. [45] pointed out that the human body is a good electrical conductor, but the electrical conductivity varies with tissue type, thickness, physiological changes, and temperature. These conditions can greatly vary from subject to subject (and even within subject). Song et al. [46] mentioned that the muscle mass varies from person to person and the EMG signal can be different for each electrode attachment position. Therefore, this may be the reason why the latter two groups of experiments did not achieve similar effects to the first group.

Nonetheless, compared with previous conclusions that EMG signal restoration is not good, the deep learning reconstruction algorithm based on TCN proposed in this paper achieves more efficient and high-quality EMG signal reconstruction when employing a single-person personalized model and this compression method provides a key+encoded signal method for transmission, which reduces the amount of data transmitted while ensuring security. Our work enables more accurate, real-time monitoring of the generated EMG signals. In clinical practice, doctors can analyze the characteristics of the EMG to determine whether muscles are damaged or diseased. .

However, there are still some limitations in this work. It may be time-consuming in practical applications since the subject-dependent model has to construct separate models for each subject. In addition, when dealing with data from large-scale populations, personalized models may not be practical

enough, as each individual needs to be processed separately. This is the problem that we need to solve in the next step.

For future expectations, firstly, we will test the method proposed in this study on a dataset with added noise and attempt to use other networks to accelerate training speed and improve reconstruction accuracy. Secondly, the review paper [25] summarized a DBBD determination matrix suitable for physiological signals proposed by Andreaniaina Ravelomanantsoa et al. [47], which can achieve good results and is easily implemented in hardware [38, 47, 48]. In paper [49], Nguyen et al. pointed out that using deterministic matrices in compressed sensing can further improve reconstruction efficiency and accuracy. In addition, the deterministic measurement matrix proposed by Wang et al. [50] has minor mutual coherence and superior reconstruction capability of CS signals. Therefore, using a deterministic-based measurement matrix for EMG signals CS is an attractive research direction. We will compare the deterministic-based measurement matrices with the random measurement matrices in future work. Thirdly, we will conduct larger-scale experiments to further optimize and even attempt to establish a universal model suitable for everyone.

CRediT authorship contribution statement

Liangyu Zhang: Investigation, Methodology, Software, Formal analysis, Data curation, Visualization, Writing – original draft. **Junxin Chen**: Methodology. **Wenyan Liu**: Writing – review. **Xiufang Liu**: Writing – editing. **Chenfei Ma**: Methodology, Software, Writing – review. **Lisheng Xu**: Methodology, Writing – review & editing.

Declaration of Competing Interest

The authors declare that they have no known competing financial interests or personal relationships that could have appeared to influence the work reported in this paper.

Acknowledgments

This work was supported by the Liaoning Provincial 'Selecting the Best Candidates by Opening Competition Mechanism' Science and Technology Program (No.2022JH/10400004). This study was also supported by the National Natural Science Foundation of China (No. 62273082 and No. 61773110),

the Natural Science Foundation of Liaoning Province (No. 20170540312 and No. 2021-YGJC-14), the Basic Scientific Research Project (Key Project) of Liaoning Provincial Department of Education (LJKZ00042021), the Fundamental Research Funds for the Central Universities (No. N2119008), and the Shenyang Science and Technology Plan Fund (No. 21-104-1-24, No. 20-201-4-10, and No. 201375).

References

[1] Ammu Anna Mathew, Arunkumar Chandrasekhar, and S Vivekanandan. A review on real-time implantable and wearable health monitoring sensors based on triboelectric nanogenerator approach. *Nano Energy*, 80:105566, 2021.

[2] Mohammadreza Balouchestani and Sridhar Krishnan. Robust compressive sensing algorithm for wireless surface electromyography applications. *Biomedical Signal Processing and Control*, 20:100–106, 2015.

[3] Valentín A Catacora, Federico N Guerrero, and Enrique M Spinelli. Three-electrode double-differential biopotential amplifier for surface emg measurements. *IEEE Transactions on Instrumentation and Measurement*, 2023.

[4] Charn Loong Ng, Mamun Bin Ibne Reaz, and Muhammad Enamul Hoque Chowdhury. A low noise capacitive electromyography monitoring system for remote healthcare applications. *IEEE Sensors Journal*, 20(6):3333–3342, 2019.

[5] Huasong Cao, Victor Leung, Cupid Chow, and Henry Chan. Enabling technologies for wireless body area networks: A survey and outlook. *IEEE Communications Magazine*, 47(12):84–93, 2009.

[6] Priyanka Bera and Rajarshi Gupta. Hybrid encoding algorithm for real time compressed electrocardiogram acquisition. *Measurement*, 91:651–660, 2016.

[7] Abbas Rohani Bastami and Sima Vahid. Estimating the size of naturally generated defects in the outer ring and roller of a tapered roller bearing based on autoregressive model combined with envelope analysis and discrete wavelet transform. *Measurement*, 159:107767, 2020.

[8] Rajesh Kumar and Manpreet Singh. Outer race defect width measurement in taper roller bearing using discrete wavelet transform of vibration signal. *Measurement*, 46(1):537–545, 2013.

[9] Mark J Shensa et al. The discrete wavelet transform: wedding the a trous and mallat algorithms. *IEEE Transactions on Signal Processing*, 40(10):2464–2482, 1992.

[10] Jian Sun, Hongru Li, and Baohua Xu. The morphological undecimated wavelet decomposition–discrete cosine transform composite spectrum fusion algorithm and its application on hydraulic pumps. *Measurement*, 94:794–805, 2016.

[11] Helder Sousa and Ying Wang. Sparse representation approach to data compression for strain-based traffic load monitoring: A comparative study. *Measurement*, 122:630–637, 2018.

[12] Chao-Yang Pang, Ri-Gui Zhou, Ben-Qiong Hu, WenWen Hu, and Ahmed El-Rafei. Signal and image compression using quantum discrete cosine transform. *Information Sciences*, 473:121–141, 2019.

[13] Hua-Ping Wan, Guan-Sen Dong, Yaozhi Luo, and Yi-Qing Ni. An improved complex multi-task bayesian compressive sensing approach for compression and reconstruction of shm data. *Mechanical Systems and Signal Processing*, 167:108531, 2022.

[14] Darren Craven, Brian McGinley, Liam Kilmartin, Martin Glavin, and Edward Jones. Compressed sensing for bioelectric signals: A review. *IEEE Journal of Biomedical and Health informatics*, 19(2):529–540, 2014.

[15] PP Vaidyanathan. Generalizations of the sampling theorem: Seven decades after nyquist. *IEEE Transactions on Circuits and Systems I: Fundamental Theory and Applications*, 48(9):1094–1109, 2001.

[16] David L Donoho. Compressed sensing. *IEEE Transactions on Information Theory*, 52(4):1289–1306, 2006.

[17] Zhuo Pang, Mei Yuan, and Michael B Wakin. A random demodulation architecture for sub-sampling acoustic emission signals in structural health monitoring. *Journal of Sound and Vibration*, 431:390–404, 2018.

[18] Afonso S Bandeira, Matthew Fickus, Dustin G Mixon, and Percy Wong. The road to deterministic matrices with the restricted isometry property. *Journal of Fourier Analysis and Applications*, 19(6):1123–1149, 2013.

[19] Scott Shaobing Chen, David L Donoho, and Michael A Saunders. Atomic decomposition by basis pursuit. *SIAM Review*, 43(1):129–159, 2001.

[20] Joel A Tropp and Anna C Gilbert. Signal recovery from random measurements via orthogonal matching pursuit. *IEEE Transactions on Information Theory*, 53(12):4655–4666, 2007.

[21] Wei Dai and Olgica Milenkovic. Subspace pursuit for compressive sensing signal reconstruction. *IEEE transactions on Information Theory*, 55(5):2230–2249, 2009.

[22] Anupriya Gogna, Angshul Majumdar, and Rabab Ward. Semi-supervised stacked label consistent autoencoder for reconstruction and analysis of biomedical signals. *IEEE Transactions on Biomedical Engineering*, 64(9):2196–2205, 2016.

[23] Alexander J Casson and Esther Rodriguez-Villegas. Signal agnostic compressive sensing for body area networks: Comparison of signal reconstructions. In *2012 Annual International Conference of the IEEE Engineering in Medicine and Biology Society*, pages 4497–4500. IEEE, 2012.

[24] Anna MR Dixon, Emily G Allstot, Daibashish Gangopadhyay, and David J Allstot. Compressed sensing system considerations for ecg and emg wireless biosensors. *IEEE Transactions on Biomedical Circuits and Systems*, 6(2):156–166, 2012.

[25] Bharat Lal, Raffaele Gravina, Fanny Spagnolo, and Pasquale Corsonello. Compressed sensing approach for physiological signals: A review. *IEEE Sensors Journal*, 2023.

[26] Mohammadreza Balouchestani and Sridhar Krishnan. Effective low-power wearable wireless surface emg sensor design based on analog-compressed sensing. *Sensors*, 14(12):24305–24328, 2014.

[27] Mohammadreza Balouchestani, Kaamran Raahemifar, and Sridhar Krishnan. New sampling approach for wireless ecg systems with compressed sensing theory. In *2013 IEEE International Symposium on Medical Measurements and Applications (MeMeA)*, pages 213–218. IEEE, 2013.

[28] Liangyu Zhang, Junxin Chen, Chenfei Ma, Xiufang Liu, and Lisheng Xu. Performance analysis of electromyogram signal compression sampling in a wireless body area network. *Micromachines*, 13(10):1748, 2022.

[29] Lorenzo Manoni, Claudio Turchetti, Laura Falaschetti, and Paolo Crippa. A comparative study of computational methods for compressed sensing reconstruction of emg signal. *Sensors*, 19(16):3531, 2019.

[30] Yong-Siang Chen, Hsin-Yi Lin, Hung-Chih Chiu, and Hsi-Pin Ma. A compressive sensing framework for electromyogram and electroencephalogram. In *2014 IEEE International Symposium on Medical Measurements and Applications (MeMeA)*, pages 1–6. IEEE, 2014.

[31] Hongpo Zhang, Zhongren Dong, Zhen Wang, Lili Guo, and Zongmin Wang. Csnet: A deep learning approach for ecg compressed sensing. *Biomedical Signal Processing and Control*, 70:103065, 2021.

[32] Mauro Mangia, Luciano Prono, Alex Marchioni, Fabio Pareschi, Riccardo Rovatti, and Gianluca Setti. Deep neural oracles for short-window optimized compressed sensing of biosignals. *IEEE Transactions on Biomedical Circuits and Systems*, 14(3):545–557, 2020.

[33] Priya Ranjan Muduli, Rakesh Reddy Gunukula, and Anirban Mukherjee. A deep learning approach to fetal-ecg signal reconstruction. In *2016 Twenty Second National Conference on Communication (NCC)*, pages 1–6. IEEE, 2016.

[34] Shaojie Bai, J Zico Kolter, and Vladlen Koltun. An empirical evaluation of generic convolutional and recurrent networks for sequence modeling. *arXiv preprint arXiv:1803.01271*, 2018.

[35] Joseph L Betthauser, John T Krall, Shain G Bannowsky, György Lévay, Rahul R Kaliki, Matthew S Fifer, and Nitish V Thakor. Stable responsive emg sequence prediction and adaptive reinforcement with temporal

convolutional networks. *IEEE Transactions on Biomedical Engineering*, 67(6):1707–1717, 2019.

[36] Joseph L Betthauser, John T Krall, Rahul R Kaliki, Matthew S Fifer, and Nitish V Thakor. Stable electromyographic sequence prediction during movement transitions using temporal convolutional networks. In *International Conference on Neural Engineering*, pages 1046–1049. IEEE, 2019.

[37] Panagiotis Tsinganos, Bruno Cornelis, Jan Cornelis, Bart Jansen, and Athanassios Skodras. Improved gesture recognition based on semg signals and tcn. In *IEEE International Conference on Acoustics, Speech and Signal Processing*, pages 1169–1173. IEEE, 2019.

[38] Andrianiaina Ravelomanantsoa, Hassan Rabah, and Amar Rouane. Compressed sensing: A simple deterministic measurement matrix and a fast recovery algorithm. *IEEE Transactions on Instrumentation and Measurement*, 64(12):3405–3413, 2015.

[39] Yong-Siang Chen, Hsin-Yi Lin, Hung-Chih Chiu, and Hsi-Pin Ma. A compressive sensing framework for electromyogram and electroencephalogram. In *2014 IEEE International Symposium on Medical Measurements and Applications (MeMeA)*, pages 1–6. IEEE, 2014.

[40] Emmanuel Candes and Justin Romberg. l1-magic: Recovery of sparse signals via convex programming. *URL: www. acm. caltech. edu/l1magic/downloads/l1magic. pdf*, 4(14):16, 2005.

[41] Alex Sherstinsky. Fundamentals of recurrent neural network (rnn) and long short-term memory (lstm) network. *Physica D: Nonlinear Phenomena*, 404:132306, 2020.

[42] Manfredo Atzori, Arjan Gijsberts, Claudio Castellini, Barbara Caputo, Anne-Gabrielle Mittaz Hager, Simone Elsig, Giorgio Giatsidis, Franco Bassetto, and Henning Müller. Electromyography data for non-invasive naturally-controlled robotic hand prostheses. *Scientific Data*, 1(1):1–13, 2014.

[43] Changcheng Wu, Aiguo Song, Yun Ling, Nan Wang, Lei Tian, et al. A control strategy with tactile perception feedback for emg prosthetic hand. *Journal of Sensors*, 2015, 2015.

[44] Yaniv Zigel, Arnon Cohen, and Amos Katz. The weighted diagnostic distortion (wdd) measure for ecg signal compression. *IEEE Transactions on Biomedical Engineering*, 47(11):1422–1430, 2000.

[45] Peter Konrad. The abc of emg. *A practical introduction to kinesiological electromyography*, 1(2005):30–5, 2005.

[46] Min-Su Song, Sung-Gu Kang, Kyu-Tae Lee, and Jeonghyun Kim. Wireless, skin-mountable emg sensor for human–machine interface application. *Micromachines*, 10(12):879, 2019.

[47] Andrianiaina Ravelomanantsoa, Amar Rouane, Hassan Rabah, Nicolas Ferveur, and Landry Collet. Design and implementation of a compressed sensing encoder: application to emg and ecg wireless biosensors. *Circuits, Systems, and Signal Processing*, 36:2875–2892, 2017.

[48] Dipayan Mitra, Hadi Zanddizari, and Sreeraman Rajan. Investigation of kronecker-based recovery of compressed ecg signal. *IEEE Transactions on Instrumentation and Measurement*, 69(6):3642–3653, 2019.

[49] Thu LN Nguyen, Yoan Shin, et al. Deterministic sensing matrices in compressive sensing: A survey. *The Scientific World Journal*, 2013, 2013.

[50] Yue Wang, Yali Qin, and Hongliang Ren. Deterministic construction of compressed sensing measurement matrix with arbitrary sizes via qc-ldpc and arithmetic sequence sets. *Electronics*, 12(9):2063, 2023.

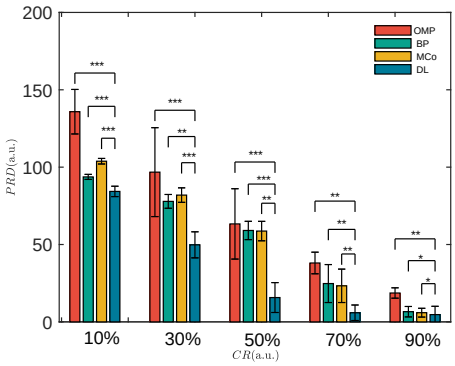

(a)

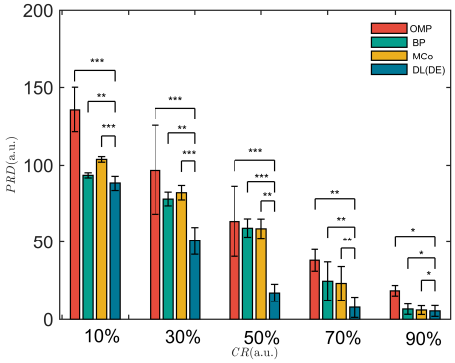

(b)

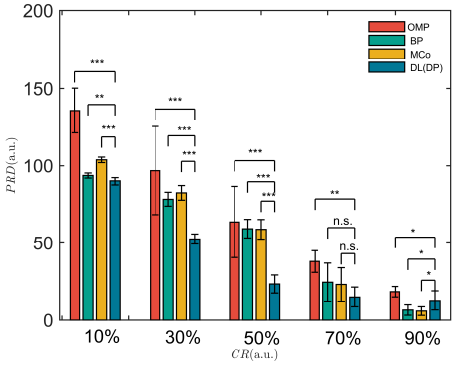

(c)

Fig. 7. PRD (mean±SD) of reconstructed signal and original signal by four reconstruction algorithms. Wilcoxon rank-sum test for differences in the PRD between groups. '*' indicates statistical significance ($p<0.05$). '**' indicates statistical significance ($p<0.01$). '***' indicates statistical significance ($p<0.001$). Not statistically significant is represented by 'n.s.'. (a),(b) and (c) are the comparison of three reconstruction algorithms with DL, DL(DE), and DL(DP), respectively.

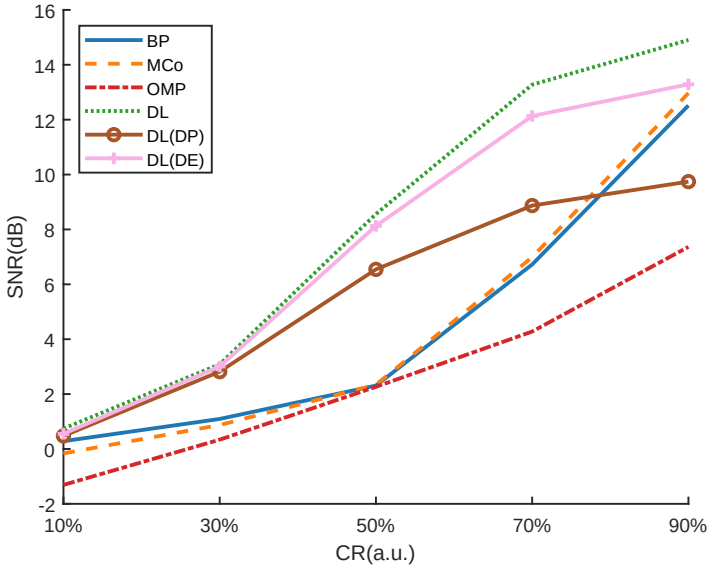

Fig. 8. Comparison of averaged SNR at different CRs.

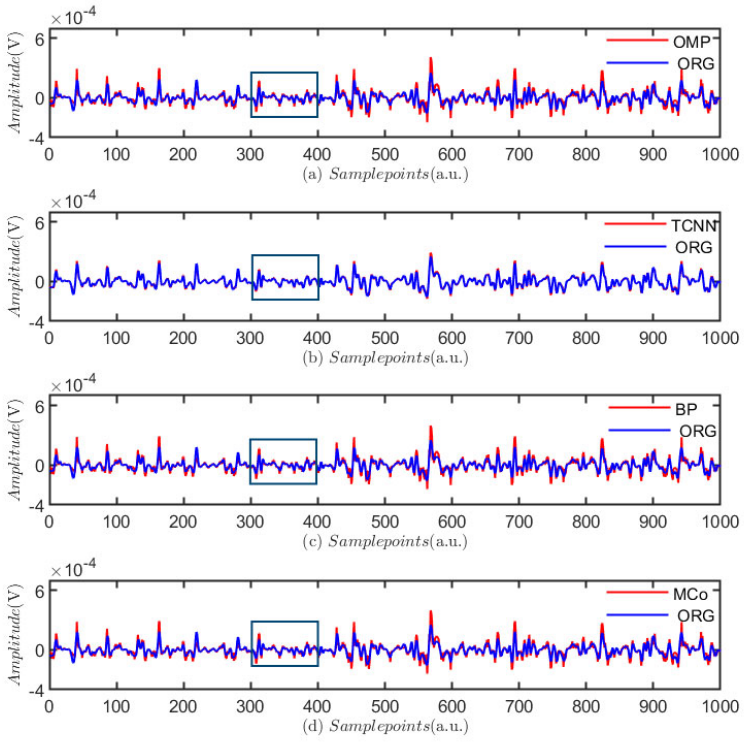

Fig. 9. Record 1 reconstructions for 0.5 seconds, when CR = 50%. (a), (b), (c) and (d) show the comparison between the original signals(ORG) and the reconstructed signals using four algorithms respectively. The training and testing sets are from the fixed position of the same subject.

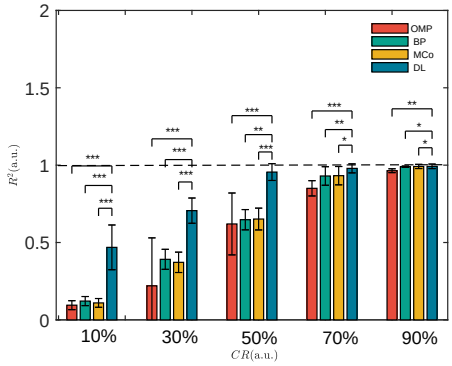

(a)

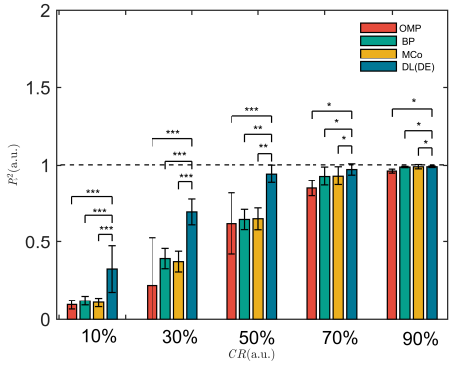

(b)

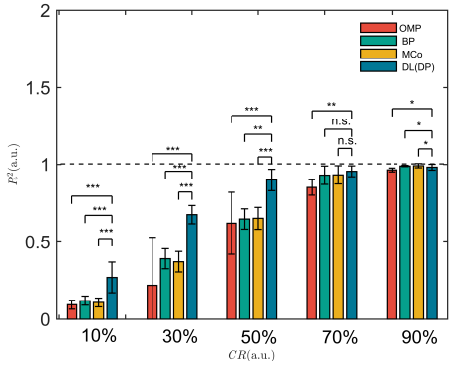

(c)

Fig. 10. R^2(mean±SD) of reconstructed signal and original signal by four reconstruction algorithms. Wilcoxon rank-sum test for differences in the coefficient of determination between groups. '*' indicates statistical significance (p<0.05). '**' indicates statistical significance (p<0.01). '***' indicates statistical significance (p<0.001). Not statistically significant is represented by 'n.s.'. (a),(b) and (c) are the comparison of three reconstruction algorithms with DL, DL(DE), and DL(DP), respectively.

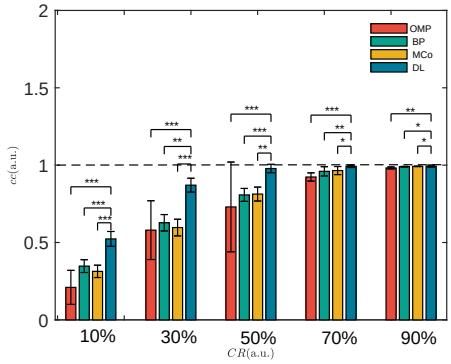

(a)

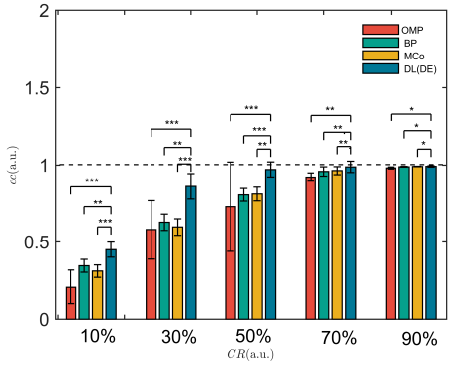

(b)

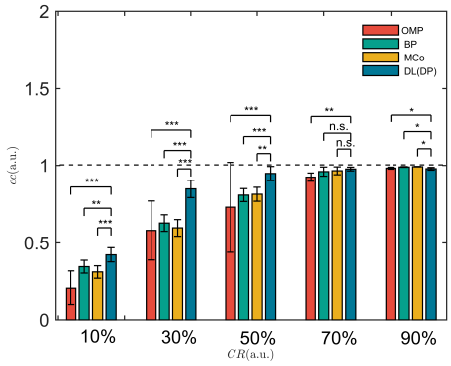

(c)

Fig. 11. r (mean ± SD) of reconstructed signal and original signal by four reconstruction algorithms. Wilcoxon rank-sum test for differences in the correlation coefficient between groups. '*' indicates statistical significance ($p<0.05$). '**' indicates statistical significance ($p<0.01$). '***' indicates statistical significance ($p<0.001$).Not statistically significant is represented by 'n.s.'. (a),(b) and (c) are the comparison of three reconstruction algorithms with DL, DL(DE), and DL(DP), respectively.